

## **Bioinformatic Studies on Buffalo Prolactin Derived Anti-Angiogenic Peptide**

Authors: Pulak P. Kumar, Pratihtha Singh

Submitted: 8. June 2016

Published: 8. June 2016

Volume: 3

Issue: 3

Keywords: Bioinformatics, buffalo prolactin, angiogenesis, molecular docking, molecular modeling, homology modeling, kallikrein-kinin system, bradykinin B1 receptor, synthetic peptide, somatostatin

DOI: 10.17160/josha.3.3.193

# JOSHA

[josha.org](http://josha.org)

**Journal of Science,  
Humanities and Arts**

JOSHA is a service that helps scholars, researchers, and students discover, use, and build upon a wide range of content

# Bioinformatic Studies on Buffalo Prolactin Derived Anti-Angiogenic Peptide

Pulak Kumar<sup>a</sup> and Pratishtha Singh<sup>b</sup>

<sup>a</sup>Faculty of Life Sciences and Biotechnology, South Asian University, New Delhi-110021, [pollock1992@gmail.com](mailto:pollock1992@gmail.com)

<sup>b</sup>School of Life Sciences, Jawaharlal Nehru University, New Delhi-110067, [rai.pratishtha86@gmail.com](mailto:rai.pratishtha86@gmail.com)

## Abstract

A 14-amino acid sequence within the buffalo prolactin (buPRL) protein has been identified by BLAST search as similar to that of somatostatin, the gold standard for determining anti-angiogenic activity. A synthetic peptide with the same sequence has been shown to exhibit powerful anti-angiogenic activity, possibly by functioning as a kallikrein-kinin system (KKS) antagonist. In order to further study this peptide's anti-angiogenic nature, bioinformatics tools were used to analyze its interaction with the bradykinin B1 receptor, which is a component of the KKS. Molecular docking studies were conducted *in silico* using structures of bradykinin B1 receptor obtained by homology modeling using SWISS-MODEL via the EXPASY web server, as well as a structure of the synthetic peptide that was modeled by the PEP-FOLD *de novo* modeling server. Docking studies were conducted with the bradykinin B1 structure using the structure of somatostatin and a PEP-FOLD derived structure of a scrambled version of the peptide. All the structures were validated using PDBsum and PROCHECK. Our results indicate that the peptide does form a complex with the bradykinin B1 receptor with a binding energy similar to that of the complex with somatostatin and the scrambled version of the peptide exhibits a similar effect. Further studies, both *in silico* and wet lab, need to be performed to provide further insights into the mechanism of this 14-amino acid peptide's anti-angiogenic activity.

## Keywords

Bioinformatics, buffalo prolactin, angiogenesis, molecular docking, molecular modeling, homology modeling, kallikrein-kinin system, bradykinin B1 receptor, synthetic peptide, somatostatin.

## Introduction

### Angiogenesis

Angiogenesis has been established as the process by which new blood vessels are formed from the pre-existing ones (Birbrair *et al.*, 2014). It is commonly known to occur in cases of animal growth, development, injury, or trauma as a steady blood supply is critical to the transportation of vital nutrients and biomolecules throughout the body. However, angiogenesis has also been known to become a major problem in cancer, as tumors can use the process of angiogenesis to grow and spread at the organism's expense (Chan-Ling 2008; Folkman 1971).

### The role of the kallikrein-kinin system (KKS) and bradykinin receptors in angiogenesis

The kallikrein-kinin system works during tissue inflammation and performs a variety of functions including cell proliferation, endothelial migration, and leukocyte activation. Evidence indicates that the system is pro-angiogenic in nature, and it functions through two cross-talking receptors, the inducible bradykinin B1 receptor (B1R) and the constitutively expressed bradykinin B2 receptor (B2R), both G-protein coupled receptors (Figure 1) (Costa, Sirois, Tannock, and Chammas, 2013).

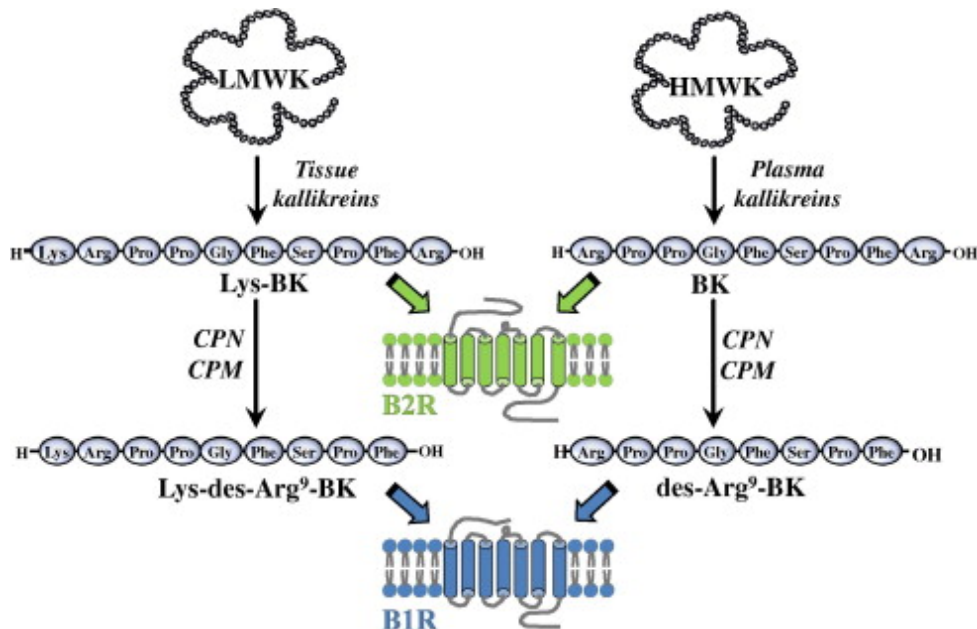


**Figure 1.** Schematic representation of the kallikrein-kinin system (adapted from Costa, Sirois, Tannock, and Chammas, 2013).

The KKS has also been implicated in cancer migration, invasion, and metastasis due to its pro-angiogenic nature and ability to increase vascular permeability. A suitable KKS antagonist could be a

vital therapeutic tool as it may counteract inflammation-related disorders and serve as an anti-cancer drug of sorts. However, only one such antagonist has successfully reached the market, Icatibant (HOE-140), a selective B2R antagonist, authorized for the treatment of hereditary angioedema (Costa, Sirois, Tannock, and Chammas, 2013).

Therefore, the aim of our study was to investigate whether a buffalo prolactin (buPRL) derived peptide, which has been shown to have anti-angiogenic properties, could act as a KKS antagonist. Our goal was to perform bioinformatics-based binding studies for a better understanding of the interaction between the peptide and the bradykinin B1 receptor.

### **Studies into the anti-angiogenic nature of peptide derivatives**

Experiments have shown that peptide derivatives of physiological proteins do display anti-angiogenic activity. For instance, D and L-peptides derived from vascular endothelial growth factor receptor 2 (VEGFR-2) inhibited its autophosphorylation at nanomolar concentrations and showed potent anti-angiogenic activity in a spheroid-based assay. This opened up the possibility of rational design of stable anti-angiogenic peptide inhibitors from their parent receptors (Piossek, *et al.*, 2003). Anti-angiogenic activity has also been demonstrated for naturally occurring Abeta peptides, which form beta-sheet aggregates that constitute a key component of senile plaques and vascular deposits in Alzheimer's disease (Paris, *et al.*, 2004).

Anti-angiogenic activity of endocrine hormone derivatives has also been shown. When the disulfide bonds of a nicked isoform of rat prolactin are reduced, the 16K N-terminal and 8K C-terminal sections are separated. The 16K N-terminal region of both rat and human prolactin were shown to display anti-angiogenic activity, both *ex vivo* and *in vivo* in rats and in humans (Ferrara, Clapp, and Weiner, 1991; Clapp, Martial, Guzman, Rentier-Delure, and Weiner, 1993). In contrast, the intact and nicked isoforms of prolactin did not show any anti-angiogenic activity (Ferrara, Clapp, and Weiner, 1991).

Another way of isolating peptide derivatives and studying them for anti-angiogenic activity was by cathepsin D digestion. The digestion of rat and human prolactin with this enzyme is reported to have produced anti-angiogenic 16K fragments (Ferrara, Clapp, and Weiner, 1991; Clapp, Martial, Guzman, Rentier-Delure, and Weiner, 1993). Although such 16K fragments were not produced from buPRL, nor were such size isoforms naturally occurring, experiments established that lower-size isoforms that were naturally occurring, when separated and purified from the monomeric protein and from each other, displayed anti-angiogenic activity (Lee, Chaudhary, and Muralidhar, 2012). Similarly, cathepsin-digested fragments of buffalo prolactin also display anti-angiogenic activity (Lee, Majumder, Chatterjee, and Muralidhar, 2011). In particular, a 14-amino acid synthetic peptide, which is based on

a region of buPRL with sequence similarity to that of somatostatin, has also shown to be anti-angiogenic (Lee, Majumder, Chatterjee, and Muralidhar, 2011) and, thus, was the focus of our study.

## Objectives

1. To approximate the 3-dimensional (3D) structures of the 14-amino acid synthetic peptide, a scrambled version of the provided synthetic peptide, and the bradykinin B1 receptor, and to obtain the 3D structure of somatostatin from the PDB database.

2. To select the most appropriate model for each of the peptides and dock them with an appropriate model of the bradykinin B1 receptor (Figure 2).

3. To refine the resultant docking complexes and select the best ones for each peptide based on free energy values and the scoring systems of the docking program used.

4. To compare the best docking complexes formed with the bradykinin B1 receptor for somatostatin, the buPRL-derived peptide, and the scrambled peptide, and discuss their implications on our understanding of how the 14-amino acid buPRL-derived peptide interacts with the bradykinin B1 receptor.

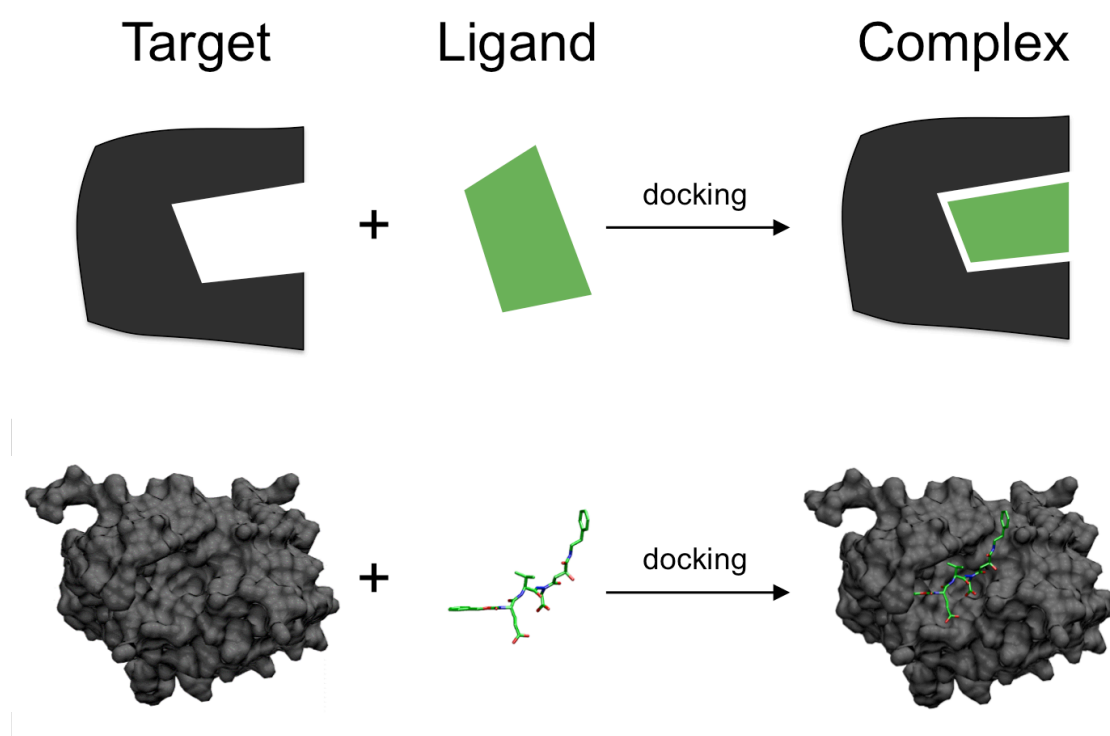


**Figure 2.** Schematic representation of the basic procedure of molecular docking. Adapted from a user-generated image on Wikipedia.

## Methods and Techniques

- PEP-FOLD 1.5, a free web server, was used for *de novo* modeling of the 14-amino acid and scrambled peptides. This server is available at the Paris Diderot University's RPBS (Ressource Parisienne en Bioinformatique Structurale) MobyLe portal (<http://bioserv.rpbs.univ-paris-diderot.fr/services/PEP-FOLD/>)(<http://mobyLe.rpbs.univ-paris-diderot.fr/cgi-bin/portal.py#forms::PEP-FOLD3>). This server allows estimation of conformations of peptides from 9 to 25 amino acids in length (Thévenet, *et al.*, 2012; Maupetit, Derreumaux, and Tuffery, 2009; Maupetit, Derreumaux, and Tufféry, 2010).

- SWISS-MODEL was accessed via the EXPASY web server (<http://swissmodel.expasy.org/>) and was used for homology modeling of bradykinin receptor. Homology modeling is the estimation of a 3D structure of a protein on the basis of an experimentally determined structure (template) that bears some homology to it (Biasini, *et al.*, 2014; Arnold, Bordoli, Kopp, and Schwede, 2006; Benkert, Biasini, and Schwede, 2011).

- Patch Dock server, beta 1.3 version, available from the BioInfo3D group at Tel Aviv University (<http://bioinfo3d.cs.tau.ac.il/PatchDock/>) was used for running shape-complementarity based docking simulations (Duhovny, Nussinov, and Wolfson, 2002; Schneidman-Duhovny, Inbar, Nussinov, and Wolfson, 2005).

- The freeware educational version of PyMol, downloaded from the Schrodinger Inc's PyMOL website (<http://pymol.org>), was used to visualize the protein structures.

- The FireDock server, also available from the BioInfo 3D group at Tel Aviv University (<http://bioinfo3d.cs.tau.ac.il/FireDock/index.html>) was used for energy analysis and refinement of docked protein results (Andrusier, Nussinov, and Wolfson, 2007).

- The RCSB (Research Collaboratory in Structural Biology) Protein Data Bank (PDB) database (<http://rcsb.org>) was used for assessing the known 3D structure of somatostatin.

- The National Centre for Biotechnology Information (NCBI) protein database (<http://www.ncbi.nlm.nih.gov/protein>) was used for obtaining the sequences of somatostatin and the bradykinin B1 receptor.

- The PDBSum web server, maintained by the European Bioinformatics Institute (EBI), (<http://www.ebi.ac.uk/thornton-srv/databases/pdbsum/>) was used for analysis, Ramachandran Plot generation, and validation of protein structure models. Specifically, PDBSum Generate was used for submission of the PDB structures of the models for analysis. This server conducted its own PROCHECK analysis for Ramachandran plot generation and validation of the submitted structures (Beer, Berka, Thornton, and Laskowski., 2014; Laskowski, *et al.*, 1997).

- For the bradykinin B1 receptor models, PROCHECK analysis and Ramachandran plot generation and validation were done via SWISS-MODEL.

## Results

The background literature and prior experiments provided the sequences for the buPRL-derived peptide (AQGKGFITMALNSC) and the scrambled peptide (TASQGFINACGMLK). The sequence of the bradykinin B1 receptor was obtained from the NCBI Protein database. The buPRL-derived peptide sequence and 3D structure of somatostatin were directly obtained from the NCBI Protein database and the RCSB PDB databases, respectively (Figure S1, Supplementary Data). There were no experimentally determined 3D structures available for any of the other peptides or the bradykinin B1 receptor.

The bradykinin B1 receptor was modeled using the SWISS-MODEL web server. The sequence was entered as input, following which the software automatically began a template search and modeled the receptor structure based on the templates with various degrees of sequence similarity with the receptor. The model that was ultimately selected had a sequence identity of 28.23, coverage of 0.83, and resolution of 2.71 Angstrom. This model was also validated by PROCHECK analysis (Figures S2-S6, Supplementary Data).

The 3D structures of both the buPRL-derived peptide and its scrambled version were obtained via the PEP-FOLD de novo modeling server. The sequences of each peptide were entered as input, and five structures were given by the server as output for each peptide. Based on PROCHECK validation, one structure was selected for each peptide to be used for molecular docking (Figures S7-S12, Supplementary Data).

Molecular docking was performed using the PatchDock web server for the interactions between Bradykinin B1 receptor and somatostatin, Bradykinin B1 receptor and buPRL-derived peptide, and Bradykinin B1 receptor and scrambled peptide. This server was chosen for its user-friendly nature, as it only requires the PDB structures of the receptor and ligand as input, and gives a set of docked complexes sorted by geometric score as output. The top ten results for each docking experiment were then sent to the FireDock web server for refinement and energy analysis. Shown below are the FireDock analyses of the binding energies of each of the docking complexes, along with a PyMOL visualization of the top-ranked docking complexes for each peptide (Figures 3-9).

Receptor	Ligand
model.pdb	2M11.pdb

Rank	Solution Number	Global Energy	Attractive VdW	Repulsive VdW	ACE	HB
1	4	-46.14	-34.76	32.81	0.88	-3.36
2	2	-32.01	-29.29	24.37	1.19	-2.33
3	10	-22.80	-26.74	12.07	-4.08	-0.63
4	6	-19.24	-20.40	13.78	-1.64	0.00
5	8	-15.78	-30.07	16.25	2.60	-1.37
6	7	-13.86	-6.48	0.65	-3.61	-0.75
7	5	4.83	-35.34	76.79	-6.64	-1.12
8	3	20.00	-32.67	97.15	-8.84	-2.33
9	9	49.12	-34.76	148.22	-6.05	-2.15
10	1	106.60	-40.70	246.96	-12.45	-2.98

**Figure 3.** FireDock results for bradykinin and somatostatin. The docking complex shown is based on the topmost result in terms of global energy.



**Figure 4.** The bradykinin and somatostatin docking complex, which was given the best free energy value according to FireDock (-46.14kJ).

Receptor	Ligand
model.pdb	prlpeptidemodel1.pdb

Rank	Solution Number	Global Energy	Attractive VdW	Repulsive VdW	ACE	HB
1	3	-48.57	-32.11	33.10	-11.33	-0.77
2	7	-39.17	-27.08	5.63	-5.92	-0.35
3	1	-29.93	-32.32	14.67	-2.47	-2.25
4	10	-29.11	-27.22	4.38	3.87	-1.38
5	2	-28.74	-32.79	17.26	-2.06	-2.34
6	9	-26.60	-25.63	44.08	-9.73	-1.00
7	8	-2.77	-4.45	1.84	4.01	-0.29
8	6	18.88	-27.39	84.37	-2.79	-1.10
9	4	22.85	-30.31	115.55	-13.16	-2.38
10	5	104.39	-35.02	238.36	-9.41	-1.89

**Figure 5.** Firedock results for bradykinin and buPRL-derived peptide. The docking complex shown is based on the topmost result in terms of global energy.



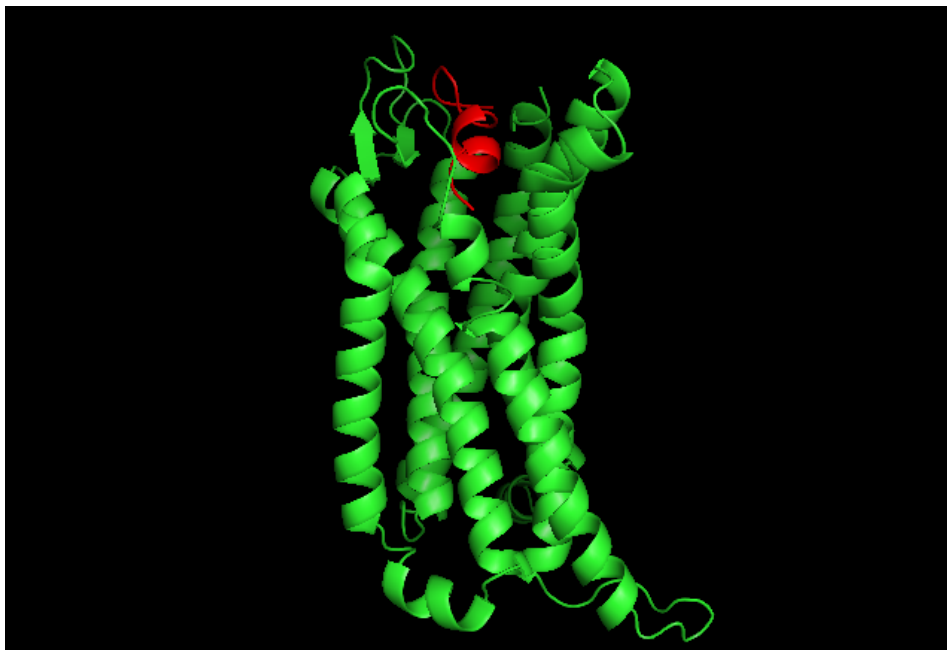


**Figure 6.** The top-scoring complex of buPRL-derived peptide and bradykinin B1 receptor, according to FireDock. Free Energy is -48.57 KJ.

Receptor		Ligand				
model.pdb		model4.pdb				
Rank	Solution Number	Global Energy	Attractive VdW	Repulsive VdW	ACE	HB
1	5	-45.81	-23.00	8.45	-4.50	-1.58
2	3	-31.80	-25.35	13.45	-6.14	-1.37
3	9	-23.52	-27.71	35.37	-6.25	-0.73
4	1	-22.19	-26.14	36.53	-5.70	-4.32
5	4	-2.96	-2.72	0.79	-0.02	0.00
6	6	-0.25	-31.58	77.48	-7.66	-0.28
7	7	5.54	-0.25	0.00	0.59	0.00
8	2	135.09	-37.89	274.17	-11.62	-0.55
9	10	217.70	-34.89	389.90	-10.94	-4.47
10	8	714.76	-51.49	1048.91	-17.92	-3.61

**Figure 7.** Firedock results for bradykinin and scrambled peptide. The docking complex shown is based on the topmost result in terms of global energy.

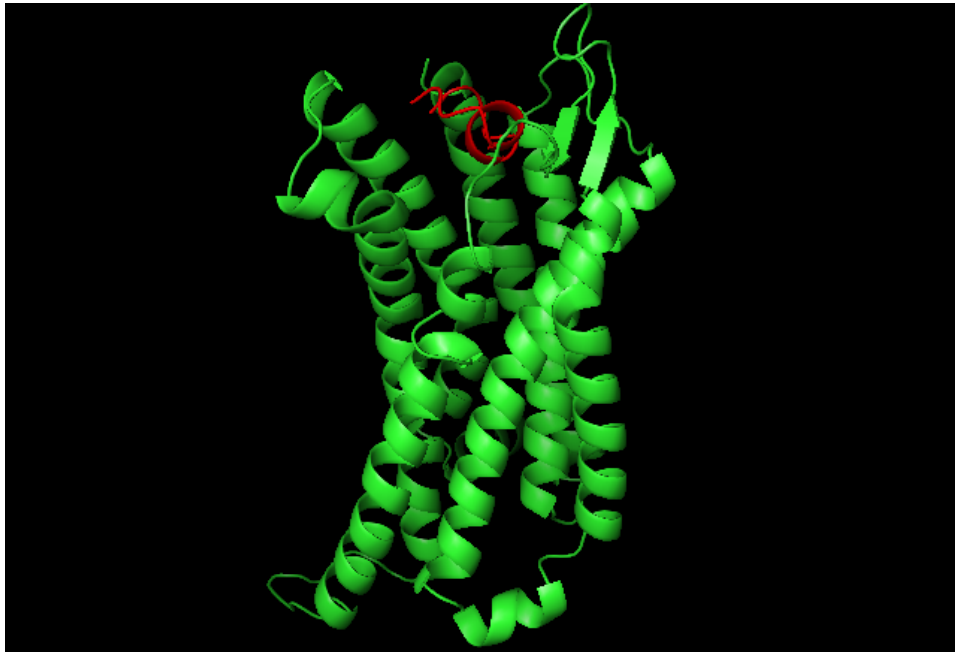


**Figure 8.** The top-ranked complex of bradykinin B1 receptor and scrambled peptide, according to FireDock. The free energy of this complex is -45.81 KJ

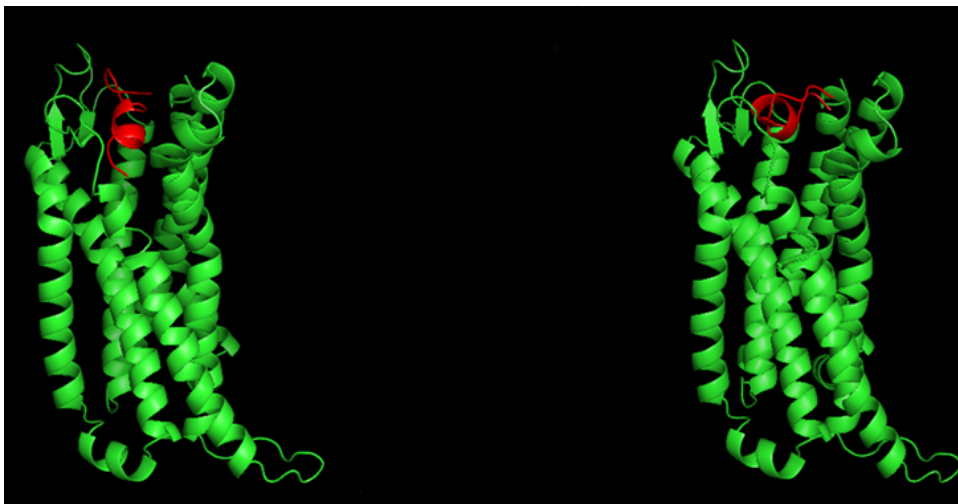


**Figure 9.** A side-by-side comparison of the docked complexes of bradykinin B1 receptor and buPRL peptide (left); and bradykinin B1 receptor and scrambled peptide (right).

## Discussion and Conclusions

Molecular docking studies between the peptides and the bradykinin B1 receptor show that the buPRL-derived peptide binds to the receptor at its active site, which is the same site where somatostatin binds. The scrambled peptide also seems to bind in the proximity of the active site, but in a different orientation. The most stable complexes formed between the bradykinin B1 receptor and each of the peptides had the following free energy values: -46.14 kJ for bradykinin B1 receptor and somatostatin, -48.57 kJ for bradykinin B1 receptor and buPRL-derived peptide, and -45.81 kJ for bradykinin B1 receptor and scrambled peptide. Though the differences in binding energies of the complexes support

the hypothesis that the buPRL-derived peptide's more potent anti-angiogenic activity is due to its stronger affinity for the bradykinin B1 receptor, these differences are also surprisingly low. The most striking inference from this would be that even the scrambled peptide would be capable of forming complexes with the bradykinin B1 receptor that would be just as stable as the complexes formed between somatostatin and the bradykinin B1 receptor. This raises many pertinent questions such as: how this scrambled peptide interacts with the bradykinin B1 receptor and what effects it could have on the kallikrein-kinin system; how will the scrambled peptide affect the physiology of an animal; does it function as a bradykinin receptor agonist or antagonist; and, finally, are its effects pro-angiogenic or anti-angiogenic? Wet lab experiments including binding assays with bradykinin receptor, as well as assays testing angiogenesis, such as the CAM assay, tube formation assay, and wound healing assay could provide some answers in this regard.

Many other questions were also raised by the findings of this study. For instance, our results contradict those of Lee *et al* (2011), which affirmed that the buPRL-derived peptide does not form a helix. According to their models, which were generated using SWISS-MODEL and Bhageerath, the 14-amino acid region within the buPRL structure that forms the basis of the synthetic peptide actually exists as a loop, and not as a helix (Jayaram, et al., 2006) (Lee, Majumder, Chatterjee, and Muralidhar, 2011). In our study, *de novo* modeling of the peptide was done using the PEP-FOLD server to see whether it retained its loop conformation when freed from its linkage to the buPRL monomer. The structure that was selected for molecular docking did not retain the loop conformation and, in fact, had a helical conformation. This opens up many avenues for discussion concerning the effect of such a conformational change on the peptide function, as the intact buPRL does not have any anti-angiogenic activity. Proper experimental determination of the structure of this peptide in solution might provide more clarity on this issue and validate the findings. Moreover, it is currently unknown whether a biomolecule similar to this synthetic peptide actually exists as a physiological protein. Using protein isolation and purification techniques, along with specific detection assays such as western blotting with an antibody specific for the synthetic peptide, would be a good way to begin the search for such a biomolecule.

The results also indicate that there are negligible conformational changes between the unbound and bound peptides, though more refined overlapping analysis needs to be done before a definite conclusion is reached. The apparent lack of a conformational change could also be a result of limitations of the shape-complementarity based approach of PatchDock.

Some concessions were made regarding experimental errors, particularly concerning the Ramachandran maps of the PEP-FOLD predicted structures of the bu-PRL derived synthetic peptide,

as none of the maps showed more than 80% of the residues in the most favored region. As PEP-FOLD attempts *de novo* modeling of peptide sequences, it is likely more error-prone than homology modeling.

Further courses of action can be taken to better ascertain the nature of the interactions between the buPRL-derived peptide, the scrambled version of the peptide, and the bradykinin B1 receptor. These include bioinformatics-driven analysis of the amino acid residues involved in receptor-peptide binding and their chemical interactions, which can be done using LigPlot<sup>+</sup> (Laskowski and Swindells, 2011) as well as wet lab experiments to test protein-protein interactions. Mutant peptides could be synthesized for such experiments to test the validity of the bioinformatics predictions in this regard.

### **Acknowledgements**

The authors would like to acknowledge Jaeok Lee and her team for their prior research on buffalo prolactin, its isoforms, and derivative peptides, whose findings served as the foundation for this project. We would like to thank our M.Sc. and Ph.D. supervisors, under whose guidance this project was done. Pulak Kumar's M.Sc. supervisor was Professor Kambadur Muralidhar, a member of the Faculty of Life Sciences and Biotechnology, South Asian University. Pratishtha Singh's Ph.D. supervisor is Sudha Cowsik, from the School of Life Sciences at Jawaharlal Nehru University. We would also like to acknowledge Dr. Evguenia Alechine, who provided editing services for this manuscript.

### **About the Authors**

Pulak Kumar is an aspiring scientist who finished his B.Sc. at Sri Venkateswara College in 2013 and his M.Sc. at the South Asian University in 2015. His primary research interests are biochemistry, biotechnology, microbiology, and molecular biology. His hobbies include comic and fictional writing, as well as video games. He is currently applying for PhD positions in U.S.A, Europe, and Australia.

Pratishtha Singh is a Ph.D. scholar working at the School of Life Sciences of Jawaharlal Nehru University. She's working in structural biology, and her areas of specialization include molecular modeling, molecular dynamics, nuclear magnetic resonance (NMR) spectroscopy, and circular dichroism techniques.

## References

- Andrusier, N., Nussinov, R., and Wolfson, H. J. (2007). FireDock: Fast Interaction Refinement in Molecular Docking. *Proteins*, 69(1), 139-59.
- Arnold, K., Bordoli, L., Kopp, J., and Schwede, T. (2006). The SWISS-MODEL workspace: a web-based environment for protein structure homology modelling. *Bioinformatics*, 22(2), 195-201.
- Beer, T. A., Berka, K., Thornton, J. M., and Laskowski, R. A. (2014, January). PDBsum additions. *Nucleic Acids Research*, 42(Database Issue), D292-D296.
- Benkert, P., Biasini, M., and Schwede, T. (2011). Toward the estimation of the absolute quality of individual protein structure models. *Bioinformatics*, 27(3), 343-350.
- Biasini, M., Bienert, S., Waterhouse, A., Arnold, K., Studer, G., Schmidt, T., Schwede, T. (2014, July 1). SWISS-MODEL: modelling protein tertiary and quaternary structure using evolutionary information. *Nucleic Acids Research*, 42(W), W252-W258.
- Birbrair, A., Zhang, T., Wang, Z.-M., Messi, M. L., Olson, J. D., Mintz, A., and Delbono, O. (2014, July 1). Type-2 pericytes participate in normal and tumoral angiogenesis. *American Journal of Physiology. Cell Physiology*, 307(1), 25-38.
- Burri, P. H., Hlushchuk, R., and Djonov, V. (2004, November). Intussusceptive angiogenesis: Its emergence, its characteristics, and its significance. *Developmental Dynamics*, 231(3), 474-488.
- Chan-Ling, T. (2008). Vasculogenesis and Angiogenesis in formation of human retinal vasculature. In J. S. Penn, and J. Penn (Ed.), *Retinal and Choroidal Angiogenesis* (pp. 119-139). Springer.
- Clapp, C., Martial, J. A., Guzman, R. C., Rentier-Delure, F., and Weiner, R. I. (1993). The 16-kilodalton N-terminal fragment of human prolactin is a potent inhibitor of angiogenesis. *Endocrinology*, 133(3), 1292-1299.
- Costa, P. L., Sirois, P., Tannock, I. F., and Chammas, R. (2013, December 11). The role of kinin receptors in cancer and therapeutic opportunities. *Cancer Letters*, 345(1), 27-38.
- Duhovny, D., Nussinov, R., and Wolfson, H. J. (2002). Efficient Unbound Docking of Rigid Molecules. *Lecture Notes in Computer Science*, 2452, 185-200.
- Ferrara, N., Clapp, C., and Weiner, R. (1991). The 16K fragment of prolactin specifically inhibits basal or fibroblast growth factor stimulated growth of capillary endothelial cells. *Endocrinology*, 129(2), 896-900.
- Folkman, J. (1971, November 18). Tumor angiogenesis: therapeutic implications. *New England Journal of Medicine*, 285(21), 1182-1186.
- Jayaram, B., Bhushan, K., Shenoy, S. R., Narang, P., Bose, S., Agrawal, P., Pandey, V. (2006). Bhageerath : An Energy Based Web Enabled Computer Software Suite for Limiting the Search Space of Tertiary Structures of Small Globular Proteins. *Nucleic Acids Research*, 34(21), 6195-6204.
- Kojima, H., Nakatsubo, N., Kikuchi, K., Kawahara, S., Kirino, Y., Nagoshi, H., Nagano, T. (1998, July 1). Detection and imaging of nitric oxide with novel fluorescent indicators: diamino fluoresceins. *Analytical Chemistry*, 70(13), 2446-2453.
- Laskowski, R. A., and Swindells, M. B. (2011, October 24). LigPlot+: Multiple Ligand-Protein Interaction Diagrams for Drug Discovery. *Journal of chemical information and modeling*, 51(10), 2778-2786.
- Laskowski, R. A., Hutchinson, E., Michie, A. D., Wallace, A. C., Jones, M. L., and Thornton, J. M. (1997, December). PDBsum: a web-based database of summaries and analyses of all PDB structures. *Trends in Biochemical Sciences*, 22(12), 488-490.

- Lee, J., Chaudhary, R., and Muralidhar, K. (2012, June). Anti-Angiogenic Activity of Naturally Occurring Lower Size Isoforms of Buffalo Pituitary Prolactin. *International Journal of Science and Technology*, 292-299.
- Lee, J., Majumder, S., Chatterjee, S., and Muralidhar, K. (2011, June). Inhibitory activity of the peptides derived from buffalo prolactin on angiogenesis. *Journal of biosciences*, 36(2), 341-354.
- Madri, J. A., Pratt, B. M., and Tucker, A. M. (1988, April). Phenotypic modulation of endothelial cells by transforming growth factor-beta depends upon the composition and organization of the extracellular matrix. *The Journal of cell biology*, 106(4), 1375-1384.
- Madri, J. A., Pratt, B. M., and Tucker, A. M. (1988, April). Phenotypic modulation of endothelial cells by transforming growth factor-beta depends upon the composition and organization of the extracellular matrix. *The journal of cell biology*, 106(4), 1375-84.
- Maupetit, J., Derreumaux, P., and Tuffery, P. (2009). PEP-FOLD: an online resource for de novo peptide structure prediction. *Nucleic Acids Research*, 37(W), W498-W503.
- Maupetit, J., Derreumaux, P., and Tufféry, P. (2010). A fast and accurate method for large-scale de novo peptide structure prediction. *Journal of Computational Chemistry*, 31(4), 726-38.
- McDougall, S. R., Anderson, A. R., and Chaplain, M. A. (2006, August 7). Mathematical modelling of dynamic adaptive tumour-induced angiogenesis: Clinical implications and therapeutic targeting strategies. *Journal of Theoretical Biology*, 241(3), 564-89.
- Niemistö, A., Dunmire, V., Yli-Harja, O., Zhang, W., and Shmulevich, I. (2005, April). Robust quantification of in vitro angiogenesis through image analysis. *IEEE transactions on medical imaging*, 24(4), 549-53.
- Paris, D., Townsend, K., Quadros, A., Humphrey, J., Sun, J., Brem, S., *et al* (2004). Inhibition of angiogenesis by Abeta peptides. *Angiogenesis*, 7(1), 75-85.
- Piossek, C., Thierauch, K.-H., Schneider-Mergener, J., Volkmer-Engert, R., Bachmann, M. F., Korff, T., . . . Germeroth, L. (2003, September). Potent inhibition of angiogenesis by D,L-peptides derived from vascular endothelial growth factor receptor 2. *Thrombosis and Haemostasis*, 90(3), 501-10.
- Prior, B. M., Yang, H. T., and Terjung, R. L. (2004, September 1). What makes vessels grow with exercise training? *Journal of applied physiology*, 97(3), 1119-1128.
- Schneidman-Duhovny, D., Inbar, Y., Nussinov, R., and Wolfson, H. J. (2005, July 1). PatchDock and SymmDock: servers for rigid and symmetric docking. *Nucleic Acids Research*, 33(W), W363-367.
- Staton, C. A., Stribbling, S. M., Tazzyman, S., Hughes, R., Brown, N. J., and Lewis, C. E. (2004, October). Current methods for assaying angiogenesis in vivo and in vitro. *International Journal of experimental pathology*, 85(5), 233-248.
- Thévenet, P., Shen, Y., Maupetit, J., Guyon, F., Derreumaux, P., and Tufféry, P. (2012). PEP-FOLD: an updated de novo structure prediction server for both linear and disulfide bonded cyclic peptides. *Nucleic Acids Research*, 40(W), W288-W293.

## Supplementary data

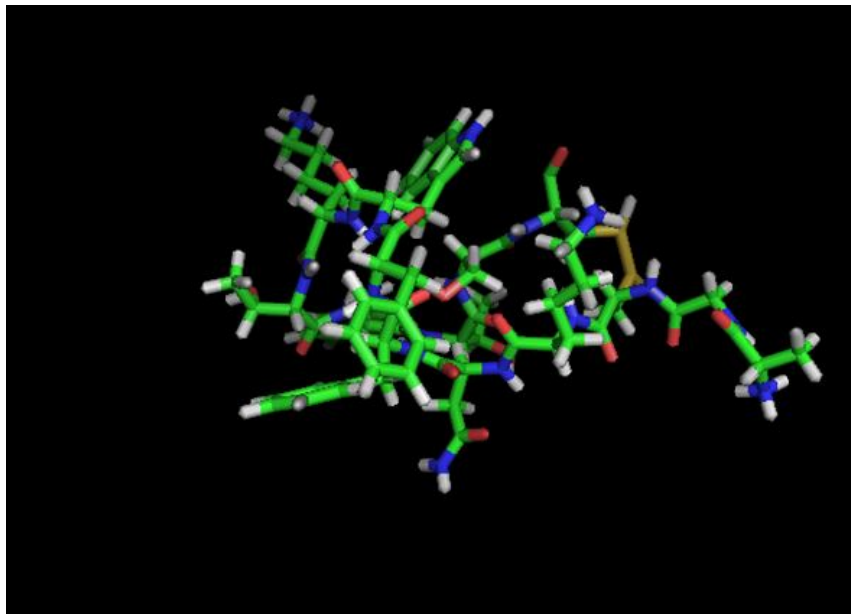



Figure S1. The 3D structure of somatostatin as seen via PyMOL.

Model #01	File	Built with	Oligo-State	Ligands	GMOE	QMEAN4
	PDB	ProMod, Version 3.70.	MONOMER	None	0.57	-6.85

QMEAN4	CR	All Atom	Solvation	Torsion
-6.8:	-4.6:	-3.1:	-3.0:	-5.1:

Templati	Seq Identity	Oligo-state	Found by	Method	Resolution	Seq Similarity	Range	Coverage	Description
4mbs.1.A	28.23	monomer	HHblits	X-ray	2.71Å	0.35	31 - 328	0.83	Chimera protein of C-C chemokine receptor type 5 and Rubredoxin

Ligand	Added to Model	Description
MRV	× - Binding site not conserved.	4,4-DIFLUORO-N-[(1S)-3-[(3-EXO)-3-(3-METHYL-5-(PROPAN-2-YL)-4H-1,2,4-TRIAZOL-4-YL)]-9-AZABICYCLO[3.2.1]OCT-8-YL]-1-PHENYLPROPYL]CYCLOHEXANECARBOXAMIDE
OLC	× - Binding site not conserved.	(2R)-2,3-DIHYDROXYPROPYL (9Z)-OCTADEC-9-ENOATE
OLC	× - Binding site not conserved.	(2R)-2,3-DIHYDROXYPROPYL (9Z)-OCTADEC-9-ENOATE
OLC	× - Binding site not conserved.	(2R)-2,3-DIHYDROXYPROPYL (9Z)-OCTADEC-9-ENOATE
OLC	× - Binding site not conserved.	(2R)-2,3-DIHYDROXYPROPYL (9Z)-OCTADEC-9-ENOATE
OLC	× - Binding site not conserved.	(2R)-2,3-DIHYDROXYPROPYL (9Z)-OCTADEC-9-ENOATE
OLC	× - Binding site not conserved.	(2R)-2,3-DIHYDROXYPROPYL (9Z)-OCTADEC-9-ENOATE
OLC	× - Binding site not conserved.	(2R)-2,3-DIHYDROXYPROPYL (9Z)-OCTADEC-9-ENOATE
ZN	× - Binding site not conserved.	ZINC ION

Figure S2. SWISS-MODEL report of the selected bradykinin B1 receptor structure.

```

Target   MASSWPPLELQSSNQSLFPQNA TACDNAPEAWDLLHRVLP TFFII SICFFGLLGNLFVLLVFLLP RRQLNVAE IYLANLA
4mbs.1.A -----N VKQIAARLL PPLYSLVF IFGFVGNMLV I L I L I N Y K R L K S M T D I Y L L N L A

Target   ASDLVFVLGLPFWAENIWNQFNW PFGALLCRVINGVIKANLFI SI FLVVA ISQDRYRVLVHPMASRRQRRRQARVT CVL
4mbs.1.A I S D L F F L L T V P F W A H Y A -- A A Q W D F G N T M C Q L L T G L Y F I G F F S G I F F I I L L T I D R Y L A V V H A V F A L K A R T V T F G V V T S V I

Target   IWVVGGLLSIPTFLLRSIQAVPDLNITACILLPHEA---WH-FARIVELNILGFLPLAAIVFFNYHILASLRTREEVS
4mbs.1.A T W V V A V F A S L P N I I F T R S Q K -- E G L H Y T C S S H F P Y S Q Y Q F W K N F Q T L K I V - I L G L V L P L L V M V I C Y S G I L K T L L R M K K Y T

Target   -----RTRCGGRKDSKTTALI L T L V V A F L V C W A P Y H F F A F L
4mbs.1.A C T V C G Y I Y N P E D G D P D N G V N P G T D F K D I P D D W V C P L C G V G K D Q F E E V E E E K K R H R D V R L I F T I M I V Y F L F W A P Y N I V L L L

Target   E F L F Q V Q A V R G C F W E D F I D L G L Q L A N F F A F T N S S L N P V I Y V F V G R L F R T K V W E L Y K Q C T P K S L A P I S S S H R K E I F Q L F W R
4mbs.1.A N T F Q E F F G L N N C S S N R L D Q A M Q V T E T L G M T H C C I N P I I Y A F V G E E F R N Y L L V F F Q K -----

Target   N
4mbs.1.A -

```

**Figure S3.** Alignment of the bradykinin B1 receptor sequence with its modeling template.

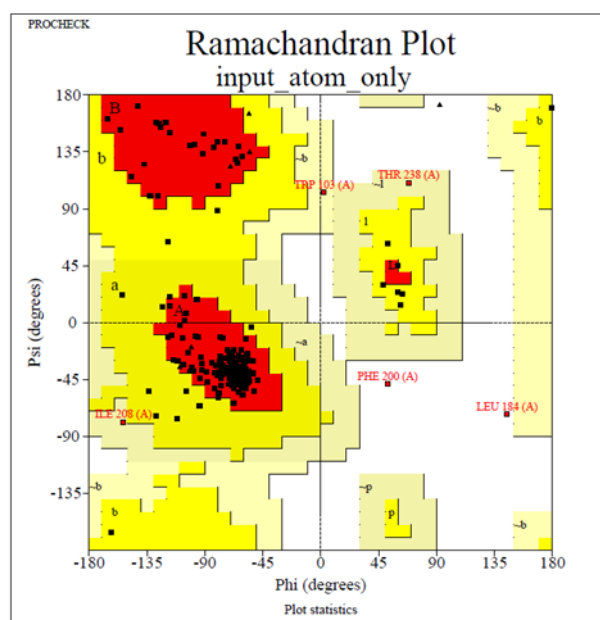


**Figure S4.** PROCHECK analysis of selected bradykinin B1 receptor model.



Residues in most favored regions [A,B,L]	246	90.4%
Residues in additional allowed regions [a,b,l,p]	21	7.7%
Residues in generously allowed regions [~a,~b,~l,~p]	3	1.1%
Residues in disallowed regions	2	0.7%
-----		
Number of non-glycine and non-proline residues	272	100.0%
Number of end-residues (excl. Gly and Pro)	2	
Number of glycine residues (shown as triangles)	13	
Number of proline residues	11	
----		
Total number of residues	298	

Based on an analysis of 118 structures of resolution of at least 2.0 Angstroms and R-factor no greater than 20%, a good quality model would be expected to have over 90% in the most favored regions.

*Figure S5. Ramachandran plot statistics of selected bradykinin B1 receptor model.*

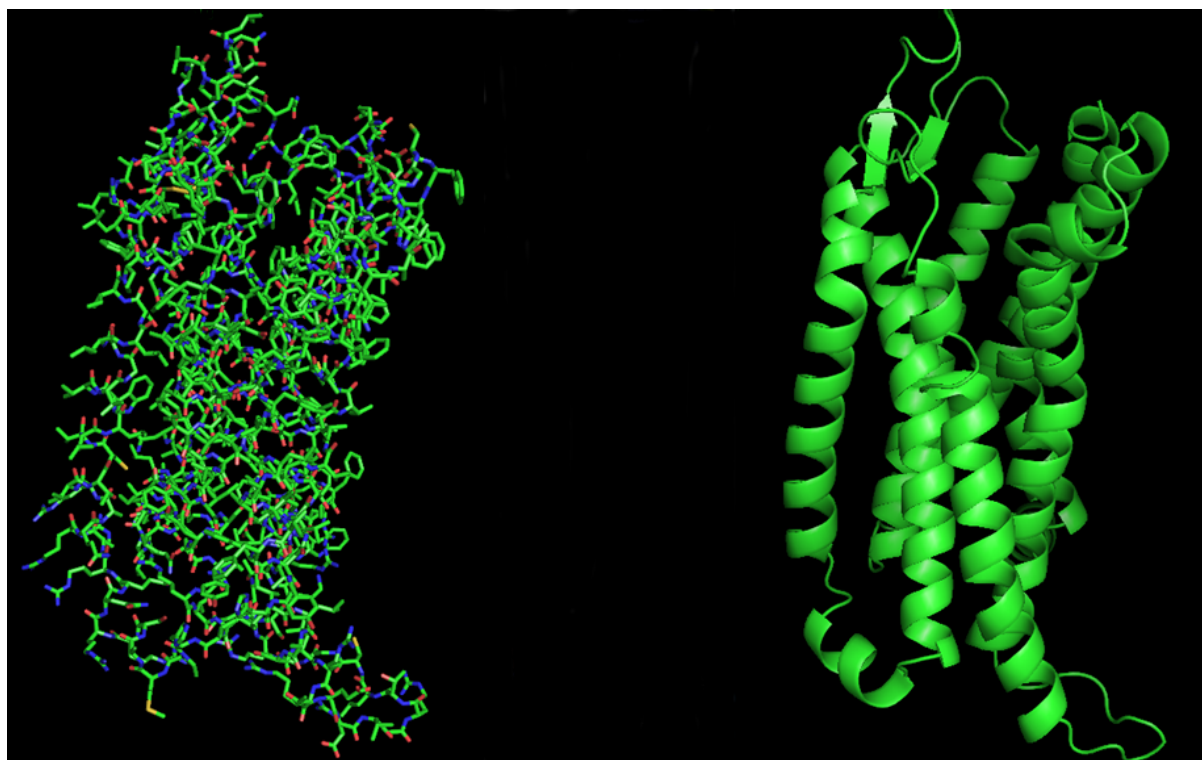


*Figure S6. 3D structure of selected bradykinin B1 receptor model in ball-and-stick form (left) and in ribbon form (right).*

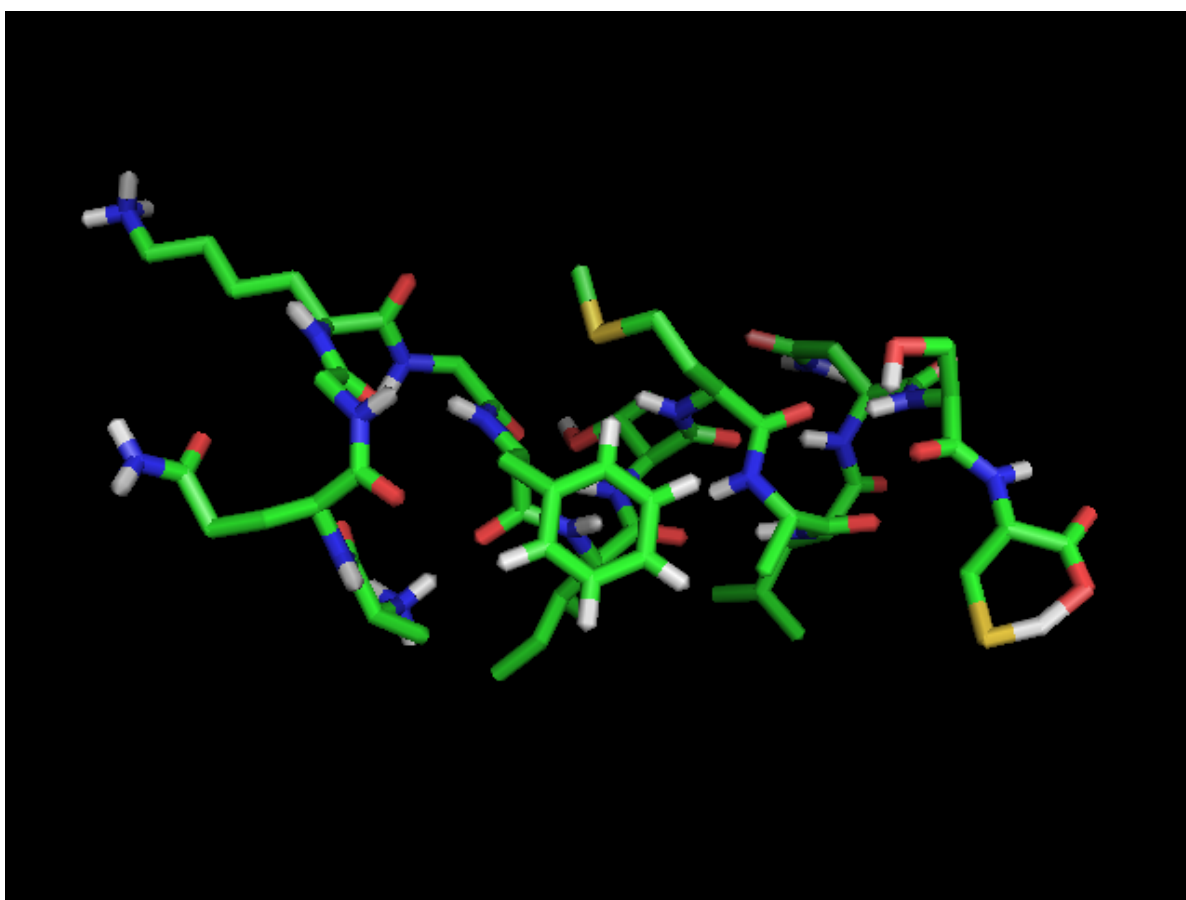


**Figure S7.** The 3D structure of the selected buPRL-derived peptide model obtained via PEP-FOLD server.

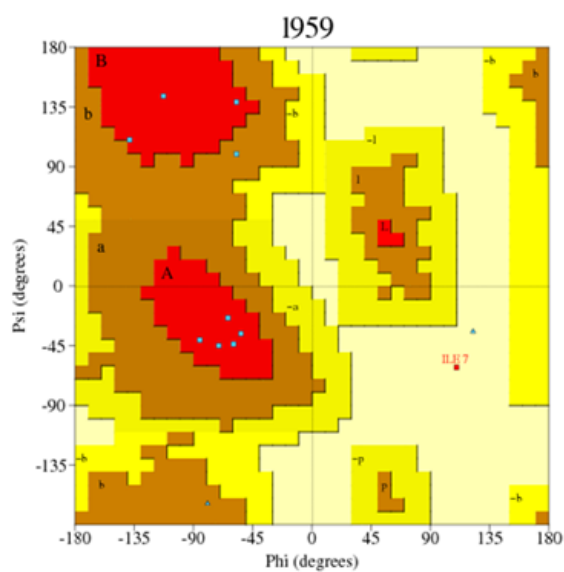


**Figure S8.** Ramachandran map obtained for buPRL-derived peptide model.

		No. of Residues	%-tage
Most favored regions	[A,B,L]	8	80.0%**
Additional allowed regions	[a,b,l,p]	1	10.0%
Generously allowed regions	[~a,~b,~l,~p]	0	0.0%
Disallowed regions	[XX]	1	10.0%**
Non-glycine and non-proline residues		10	100.0%
End-residues (excl. Gly and Pro)		2	
Glycine residues		2	
Proline residues		0	
Total number of residues		14	

Based on an analysis of 118 structures of resolution of at least 2.0 Angstroms and *R*-factor no greater than 20.0, a good quality model would be expected to have over 90% in the most favored regions [A, B, L].

*Figure S9. Ramachandran plot statistics for buPRL-derived peptide model.*

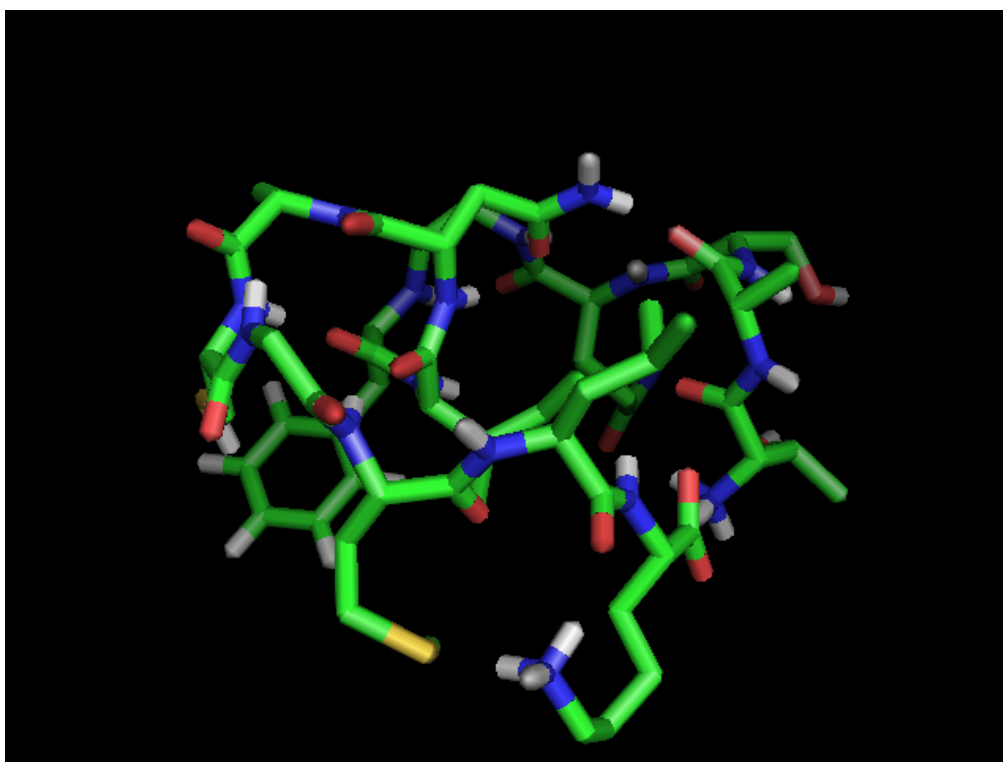


*Figure S10. 3D structure of the selected model of the scrambled version of the peptide.*

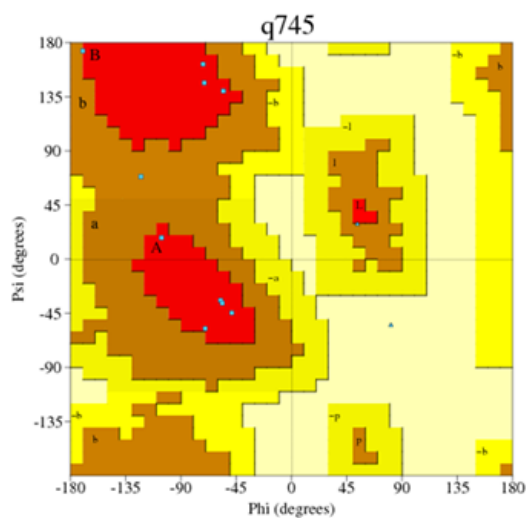


**Figure S11.** Ramachandran map for the selected scrambled peptide model.

		No. of residues	%-tage
Most favored regions	[A,B,L]	9	90.0%*
Additional allowed regions	[a,b,l,p]	1	10.0%
Generously allowed regions	[~a,~b,~l,~p]	0	0.0%
Disallowed regions	[XX]	0	0.0%
Non-glycine and non-proline residues		10	100.0%
End-residues (excl. Gly and Pro)		2	
Glycine residues		2	
Proline residues		0	
Total number of residues		14	

Based on an analysis of 118 structures of resolution of at least 2.0 Angstroms and *R*-factor no greater than 20.0, a good quality model would be expected to have over 90% in the most favored regions [A, B, L].

**Figure S12.** Ramachandran plot statistics for the selected scrambled peptide model.